

# Nucleotide Excision Repair-dependent DNA Double-strand Break Formation and ATM Signaling Activation in Mammalian Quiescent Cells\*

Received for publication, July 4, 2014, and in revised form, August 25, 2014. Published, JBC Papers in Press, August 27, 2014, DOI 10.1074/jbc.M114.589747

Mitsuo Wakasugi<sup>†1</sup>, Takuma Sasaki<sup>†1</sup>, Megumi Matsumoto<sup>‡</sup>, Miyuki Nagaoka<sup>‡</sup>, Keiko Inoue<sup>‡</sup>, Manabu Inobe<sup>‡</sup>, Katsuyoshi Horibata<sup>§2</sup>, Kiyoji Tanaka<sup>§</sup>, and Tsukasa Matsunaga<sup>‡3</sup>

From the <sup>†</sup>Faculty of Pharmacy, Institute of Medical, Pharmaceutical and Health Sciences, Kanazawa University, Kakuma-machi, Kanazawa 920-1192, Japan and the <sup>§</sup>Human Cell Biology Group, Graduate School of Frontier Biosciences, Osaka University, 1-3 Yamadaoka, Suita, Osaka 565-0871, Japan

**Background:** In quiescent human cells, UV induces histone H2AX phosphorylation by ATR in a nucleotide excision repair (NER)-dependent manner.

**Results:** UV also activates ATM in response to NER-mediated DNA double-strand break (DSB).

**Conclusion:** The NER reaction in quiescent cells potentially generates multiple types of secondary DNA damage.

**Significance:** This work highlights the importance of our understanding of the DNA damage response in quiescent cells.

Histone H2A variant H2AX is phosphorylated at Ser<sup>139</sup> in response to DNA double-strand break (DSB) and single-stranded DNA (ssDNA) formation. UV light dominantly induces pyrimidine photodimers, which are removed from the mammalian genome by nucleotide excision repair (NER). We previously reported that in quiescent G<sub>0</sub> phase cells, UV induces ATR-mediated H2AX phosphorylation plausibly caused by persistent ssDNA gap intermediates during NER. In this study, we have found that DSB is also generated following UV irradiation in an NER-dependent manner and contributes to an earlier fraction of UV-induced H2AX phosphorylation. The NER-dependent DSB formation activates ATM kinase and triggers the accumulation of its downstream factors, MRE11, NBS1, and MDC1, at UV-damaged sites. Importantly, ATM-deficient cells exhibited enhanced UV sensitivity under quiescent conditions compared with asynchronously growing conditions. Finally, we show that the NER-dependent H2AX phosphorylation is also observed in murine peripheral T lymphocytes, typical nonproliferating quiescent cells *in vivo*. These results suggest that *in vivo* quiescent cells may suffer from NER-mediated secondary DNA damage including ssDNA and DSB.

To respond to numerous genotoxic stresses, cells have developed sophisticated signal transduction pathways that are collectively known as DNA damage response (DDR)<sup>4</sup> (1–3). The

DDR senses DNA damage and activates various cellular mechanisms such as DNA repair, cell cycle checkpoint, and apoptosis. It has been becoming clear that a wide variety of covalent histone modifications are involved in DDR (4, 5). One of the best characterized examples is the phosphorylation of histone H2AX, a variant form of the core histone H2A (6). The H2AX has a conserved SQ motif known to be a target for the phosphoinositide 3-kinase-related protein kinases. In humans, the serine 139 residue within this motif is rapidly phosphorylated in response to DNA double-strand breaks (DSB), which is mainly mediated by ATM (ataxia-telangiectasia mutated), although DNA-PK (DNA-dependent protein kinase) redundantly functions. The phosphorylated H2AX ( $\gamma$ H2AX) plays a pivotal role in recruiting various DDR factors such as MDC1 around DSB sites and amplifying the DDR signaling.

Although UV light from germicidal lamps (254 nm) dominantly produces cyclobutane pyrimidine dimers (CPDs) and 6-4 photoproducts (6-4PP) but not DSB directly (7), UV exposure also induces H2AX phosphorylation triggered by single-stranded DNA (ssDNA) regions formed by at least two different mechanisms. One is S phase-dependent and is initiated by replication arrest (8–10). The second type of UV-induced H2AX phosphorylation is observed outside the S phase and depends on nucleotide excision repair (NER) (11–14). The NER-dependent H2AX phosphorylation is much more profound in quiescent G<sub>0</sub> phase compared with cycling G<sub>1</sub> phase cells (14). Recently, it has been also reported that ssDNA breaks by Ape1 endonuclease might initiate H2AX phosphorylation in non-cycling cells exposed to UV (15). In all cases, UV-induced H2AX phosphorylation is triggered by secondary DNA lesions (*i.e.* ssDNA regions) and mediated by ATR (ATM- and Rad3-related), but not ATM.

The NER-mediated secondary DNA damage formation in quiescent cells would be a serious problem specifically *in vivo*,

\* This work was supported by Grants 21510055 and 24510068 from the Ministry of Education, Culture, Sports, Science and Technology of Japan and also grants from Hokkoku Cancer Foundation (to T. M.) and Takeda Science Foundation (to M. W.).

<sup>1</sup> Both authors contributed equally to this work.

<sup>2</sup> Present address: Div. of Genetics and Mutagenesis, National Institute of Health Sciences, Tokyo 158-8501, Japan.

<sup>3</sup> To whom correspondence should be addressed: Faculty of Pharmacy, Institute of Medical, Pharmaceutical and Health Sciences, Kanazawa University, Kakuma-machi, Kanazawa 920-1192, Japan, Tel.: 81-76-234-4487; Fax: 81-76-234-4427; E-mail: matsukas@p.kanazawa-u.ac.jp.

<sup>4</sup> The abbreviations used are: DDR, DNA damage response; NER, nucleotide excision repair; DSB, DNA double-strand break; ssDNA, single-

stranded DNA; CPD, cyclobutane pyrimidine dimer; 6-4PP, 6-4 photoproducts; Ape1, apurinic/apyrimidinic endonuclease 1; XP, xeroderma pigmentosum; Ara-C, cytosine- $\beta$ -D-arabinofuranoside.

because the majority of *in vivo* cells are known to be quiescent or quiescent-like. The NER is a universal and versatile repair mechanism for removing various helix-distorting DNA lesions such as UV-induced CPD and 6-4PP, as well as chemical-induced bulky base adducts (16). The NER reaction consists of multiple steps including lesion recognition, local unwinding around a lesion, dual incisions, removal of a lesion-containing oligonucleotide (~30 nucleotides), gap-filling DNA synthesis, and ligation to parental DNA (17), which require more than 30 polypeptides in an *in vitro* reconstitution (18). Defects in the preincision step of NER cause a genetically inherited cancer-prone disease, xeroderma pigmentosum (XP), characterized by a hypersensitivity to UV light and a high incidence of skin cancer in sun-exposed area (19). The NER-deficient XP patients are genetically classified into seven different complementation groups (XP-A through XP-G) depending on which NER gene contains causal mutation. Under quiescent conditions, primary fibroblasts derived from XP-A, XP-C, and XP-G patients exhibited no H2AX phosphorylation after UV exposure (14), clearly indicating its dependence on NER reaction rather than one particular NER factor. Based on the recruitment of RPA (replication protein A) and ATRIP (ATR interacting protein) to locally damaged sites, as well as the strong enhancement of NER-dependent H2AX phosphorylation by cytosine- $\beta$ -D-arabino-furanoside (Ara-C) treatment, we proposed a model in which persistent ssDNA gaps caused by uncoupling of dual incision and gap-filling DNA synthesis might induce ATR-mediated H2AX phosphorylation. Correspondingly, quiescent cells exhibited low levels of DNA polymerase  $\delta$  and  $\epsilon$  catalytic subunits and PCNA (proliferating cell nuclear antigen) involved in the gap-filling reaction.

In this study, we have characterized the NER-dependent secondary DNA damage initiating H2AX phosphorylation in quiescent cells in more detail and tested the possibility of its formation in quiescent cells *in vivo*. We show that, in addition to ssDNA gaps, DSB is generated in an NER-dependent manner following UV, leading to the activation of ATM signaling pathways. Importantly, the activated ATM signaling partly contributes to UV resistance in human quiescent cells. We further show that UV-irradiated peripheral T lymphocytes cause NER-dependent H2AX phosphorylation, suggesting the applicability of our model to quiescent cells *in vivo*.

## EXPERIMENTAL PROCEDURES

**Cell Culture and UV Irradiation**—Human primary fibroblasts, TIG-120 (Normal), XP2BI (XP-G) and AT2KY (A-T), and hTERT-transformed cell lines, SuSa/T-n (Normal), XP3OS/T-n (XP-A) and AT1OS/T-n (A-T), were obtained as described previously (14) and cultured in Dulbecco's modified Eagle's medium (Sigma) supplemented with 10% FBS and 50  $\mu$ g/ml gentamicin in a 37 °C incubator at 5% CO<sub>2</sub>. For G<sub>0</sub> synchronization, the cells were cultured in normal medium for 4 days to near confluency and subsequently in the medium containing 1% FBS for a further 3 or 4 days. Under the quiescent condition, labeling indexes were less than 1% in all cell strains used in this study. UV irradiation was performed with germicidal lamps (Toshiba, Tokyo, Japan) as described previously (14).

In a clonogenic survival assay, appropriate numbers of asynchronously growing or G<sub>0</sub>-arrested SuSa/T-n and AT1OS/T-n cells were plated into 60-mm dishes in triplicate per each sample and incubated for 6 h to attach to the dishes. After washing with PBS(-) twice, the cells were irradiated with various doses of UV and incubated for 2–3 weeks. The colonies formed were fixed with ethanol, stained with 5% Giemsa solution, and counted under a stereomicroscope (Olympus, Tokyo, Japan).

**Antibodies and Chemicals**—Specific antibodies used in this study were anti-MRE11 (Gene Tex, Irvine, CA), anti-NBS1 (Oncogene Science, Cambridge, MA), anti-MDC1 (Bethyl Laboratories, Montgomery, TX), anti-phospho-H2AX (Ser<sup>139</sup>; Cell Signaling, Danvers, MA; Upstate, Temecula, CA), anti-phospho-ATM (Ser<sup>1981</sup>; Epitomics, Burlingame, CA), anti-phospho-Chk2 (Thr<sup>168</sup>; Cell Signaling), anti-ssDNA (Immuno-Biological Laboratories, Gunma, Japan), anti-polymerase  $\delta$  125-kDa CS and anti-polymerase  $\epsilon$  258-kDa CS (BD Biosciences, San Jose, CA), anti-PCNA (Merck), and anti- $\beta$ -actin (Bio Vision, Milpitas, CA). Anti-53BP1 antibody was kindly provided by Dr. Kuniyoshi Iwabuchi (Kanazawa Medical University, Kanazawa, Japan). The PI3K inhibitor LY294002 was purchased from Sigma. The ATM inhibitor KU-55933 and the DNA-PK inhibitor NU7026 were obtained from Abcam (Cambridge, UK). These inhibitors were dissolved in DMSO and used at the indicated concentration.

**Immunofluorescence Staining**—Immunofluorescence staining was performed essentially as described previously (14). Cells were fixed either in methanol/acetone (1:1) at -20 °C for 10 min or 4% formaldehyde at room temperature for 15 min. In the latter case, the fixed cells were further permeabilized with 0.5% Triton X-100 in 10 mM PBS (pH 7.4) at room temperature for 5 min. For ssDNA staining, cells were treated with 10 mM PBS (pH 7.4) containing 0.2% Triton X-100 on ice before fixation. After blocking with 20% FBS in 10 mM PBS (pH 7.4), cells were treated with appropriate primary antibody and subsequently Alexa Fluor<sup>TM</sup> 488 goat anti-mouse IgG (H+L) conjugate or Alexa Fluor<sup>TM</sup> 488 goat anti-rabbit IgG (H+L) conjugate (Molecular Probes, Eugene, OR). For the co-detection of UV-induced DNA damage, the stained cells were refixed with 2% formaldehyde and treated with 2 M HCl to denature their DNA. The cells were sequentially labeled either with anti-CPD monoclonal antibody (TDM-2) (20) and Alexa Fluor 594 goat anti-mouse IgG2a conjugate (Molecular Probes) or with anti-6-4PP monoclonal antibody (64M-5) (20) and Alexa Fluor 594 goat anti-mouse IgG conjugate (Molecular Probes). DAPI (Molecular Probes) was used for nuclear counterstaining. Fluorescence images were obtained with an all-in-one fluorescence microscope BZ-9000 (Keyence, Osaka, Japan) or confocal laser scanning microscope LSM710 (Carl Zeiss, Jena, Germany).

**Western Blotting**—Cells were lysed in Nonidet P-40 lysis buffer (50 mM Tris-HCl, pH 7.5, 150 mM NaCl, 1% Nonidet P-40) supplemented with protease inhibitor mixture (Roche Applied Science) and phosphatase inhibitor cocktails 1 and 2 (Sigma) or SDS sample buffer (125 mM Tris, 4% SDS, 20% glycerol, 0.01% bromophenol blue, 10%  $\beta$ -mercaptoethanol). Cell lysates were subjected to SDS-polyacrylamide gel electrophoresis and blotted onto Immobilon-P membrane (Merck). After blocking with 0.5% skim milk in PBS-T (10 mM PBS, pH 7.4,

## NER-dependent DSB Formation and ATM Activation in G<sub>0</sub> Phase

0.05% Tween 20), the membranes were incubated with specific antibodies listed above and subsequently with horseradish peroxidase-conjugated anti-mouse or anti-rabbit IgG (Thermo Fisher, Rockford, IL). Following a chemiluminescence reaction with the Immobilon western chemiluminescent HRP substrate (Merck Millipore), protein bands were visualized using a LAS4000 lumino-image analyzer and quantified with Multi Gauge software version 3.0 (GE Healthcare, Pittsburgh, PA) or Image Studio Analysis software version 4.0 (LI-COR, Lincoln, NE).

**DSB Detection**—DSB formation was analyzed by the neutral comet assay according to the manufacturer's protocol (Comet assay kit; Trevigen, Gaithersburg, MD). After UV irradiation, SuSa/T-n or XP3OS/T-n cells were trypsinized and resuspended in PBS(−) at  $2 \times 10^5$ /ml. Cells were mixed with molten agarose and transferred onto glass slides. The slides were immersed in prechilled lysis solution for 30 min, followed by equilibration in  $1 \times$  Tris borate-EDTA (TBE) buffer for 15 min. The samples were electrophoresed at 20 V for 20 min in  $1 \times$  TBE and stained with SYBR Green I. Images were obtained with an all-in-one fluorescence microscope BZ-9000, and tail moment was measured in at least 100 cells using a CometScore™ program (TriTek Corp., Sumerduck, VA).

**Isolation of T Lymphocytes and Flow Cytometric Analysis**—Thymus and lymph nodes were isolated from wild-type or xpa knock-out C57BL/6 mice. The animal experiments were approved by the animal care and use committee of Kanazawa University and conducted in compliance with its guidelines. T lymphocytes were purified by removing B cells using Dynabeads M-450 sheep anti-mouse IgG (H+L) (DynaL Biotech, Oslo, Norway). The isolated T lymphocytes were irradiated with UV or treated with etoposide (Sigma) and cultured in RPMI 1640 medium supplemented with 10% heat-inactivated FBS and 50  $\mu$ g/ml gentamicin in a 37 °C incubator at 5% CO<sub>2</sub>. Flow cytometric analyses of H2AX phosphorylation were performed with anti- $\gamma$ H2AX antibody as described previously (14).

## RESULTS

**Activation of ATM Signaling in Quiescent Human Cells following UV Irradiation**—In the previous study, we observed NER-dependent accumulation of 53BP1 in locally UV-irradiated subnuclear regions of quiescent cells (14). 53BP1 is one of the DDR factors involved in DSB signaling and co-localizes with  $\gamma$ H2AX foci following ionizing radiation (21). In this study, we have first tested whether other DSB signaling factors accumulate after local UV irradiation. Human primary fibroblasts (TIG-120) were arrested in the G<sub>0</sub> phase by a combination of contact inhibition and serum starvation and locally irradiated with UV through an isopore membrane filter. The immunofluorescence staining with specific antibodies revealed the accumulation of MRE11 (meiotic recombination 11), NBS1 (Nijmegen breakage syndrome 1), and MDC1 (mediator of DNA damage checkpoint protein 1) 1 h post-UV (Fig. 1A). In clear contrast, NER-deficient XP2BI (XP-G) cells failed to exhibit the local accumulation of those DDR factors, suggesting that these responses are mediated by NER, but not directly by UV.

We next asked whether ATM kinase is activated following UV irradiation under quiescent conditions. G<sub>0</sub>-arrested TIG-120 cells were irradiated with UV, and their lysates were recovered after 1–4 h of incubation. Western blot analysis with phospho-specific antibodies revealed that ATM Ser<sup>1981</sup> and Chk2 Thr<sup>68</sup> are phosphorylated at 1 h following UV, whereas  $\gamma$ H2AX formation was gradually increased up to 4 h (Fig. 1B). Again, the phosphorylation of ATM and Chk2 was not observed in NER-deficient XP2BI cells (Fig. 1B). To confirm the NER dependence of the phosphorylation reaction, we performed a dose-response type of experiment using other NER-deficient cell line, XP3OS/T-n, which was derived from an XP-A patient and immortalized by hTERT introduction (22). An NER-proficient control cell line, SuSa/T-n, exhibited UV dose-dependent increase of ATM and Chk2 phosphorylation ranging 10–40 J/m<sup>2</sup>, whereas NER-deficient XP3OS/T-n cells showed only marginal phosphorylation (Fig. 1C). In addition, ectopic expression of Myc-tagged XPA complemented the inability of UV-irradiated XP3OS/T-n cells to repair 6-4PP as well as to induce the phosphorylation of ATM and Chk2 (Fig. 1D). These results clearly indicate that in quiescent cells, ATM signaling is activated within 1 h after UV in an NER-dependent manner.

We further analyzed whether the NER-dependent accumulation of DDR factors depends on ATM activation. AT2KY cells from an A-T patient were arrested in G<sub>0</sub> phase by contact inhibition/serum starvation and pretreated with a PI3K inhibitor LY294002 to inhibit DNA-PK activity, because DNA-PK functions redundantly in the absence of ATM (23). AT2KY cells have no full-length ATM (24) and showed no signals of phosphorylated ATM at Ser<sup>1981</sup> following ionizing radiation, whereas their NER activity is completely normal.<sup>5</sup> Under ATM- and DNA-PK-defective conditions, we failed to observe the local accumulation of MRE11, NBS1, and 53BP1 after micro-pore UV irradiation (Fig. 2A), suggesting that the recruitment of DDR factors depends on ATM and/or DNA-PK activity. To examine their implication separately, we decided to employ specific inhibitors for ATM (KU-55933) and DNA-PK (NU7026). As expected, the treatment with KU-55933, but not NU7026, fully suppressed UV-induced phosphorylation of ATM and Chk2 (Fig. 2B). We evaluated the impacts of the two inhibitors on MRE11 accumulation in UV-irradiated subnuclear regions, which were monitored with anti-CPD antibody. As shown in Fig. 2C, KU-55933, but not NU7026, significantly impaired the local accumulation of MRE11, suggesting that ATM kinase plays a dominant role in the efficient recruitment of DDR factors.

**NER-dependent DSB Formation in Quiescent Human Cells following UV Irradiation**—Having observed the activation of ATM kinase, as well as ATM-dependent recruitment of DDR factors, we next tried to detect DSB in UV-irradiated quiescent cells using the comet assay. The NER-proficient human cell line SuSa/T-n was arrested in G<sub>0</sub> phase and irradiated with 10–40 J/m<sup>2</sup> of UV. After 1-h incubation, the cells were subjected to the neutral comet assay, and tail moment was measured as described under “Experimental Procedures.” As shown in Fig. 3

<sup>5</sup> T. Sasaki and T. Matsunaga, unpublished data.

## NER-dependent DSB Formation and ATM Activation in G<sub>0</sub> Phase

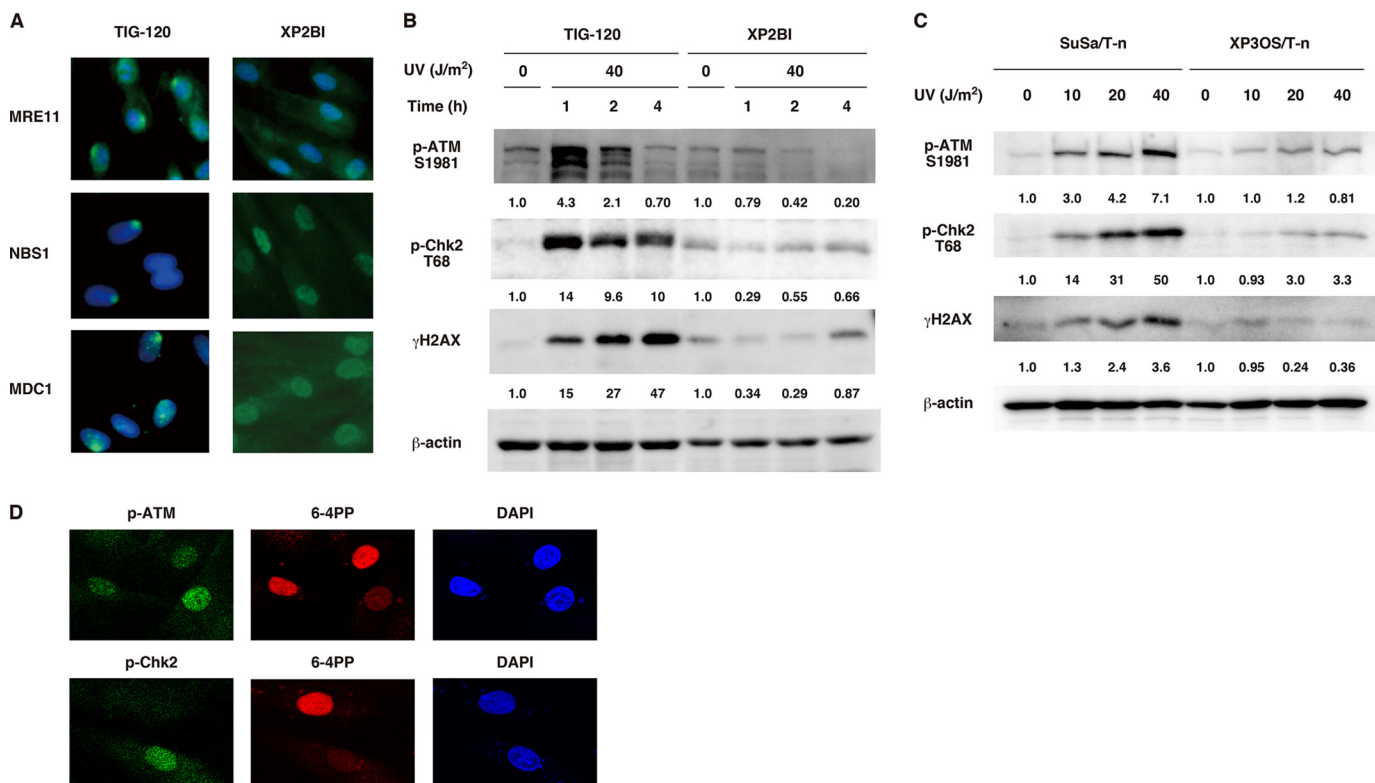


**FIGURE 1. NER-dependent recruitment of DDR factors and ATM activation in quiescent human cells.** A, TIG-120 or XP2BI cells were arrested in the G<sub>0</sub> phase by contact inhibition/serum starvation and locally irradiated with 40 J/m<sup>2</sup> of UV through an isopore membrane filter (pore size, 8 μm). After 1-h incubation, cells were fixed and stained with the indicated antibodies and DAPI. B, G<sub>0</sub>-arrested TIG-120 or XP2BI cells were irradiated with 40 J/m<sup>2</sup> of UV and incubated for up to 4 h. Cell lysates were prepared and analyzed by Western blotting with the indicated antibodies. The relative signal intensities to unirradiated control were determined by Multi Gauge software and shown in the figure. C, G<sub>0</sub>-arrested SuSa/T-n or XP3OS/T-n cells were irradiated with 10–40 J/m<sup>2</sup> of UV. After 1-h incubation, cell lysates were prepared and analyzed by Western blotting as described above. D, XP3OS/T-n cells were transfected with pCMV-Myc-XPA plasmid using FuGENE HD transfection reagent (Promega) and arrested in the G<sub>0</sub> phase by contact inhibition/serum starvation. At 2 h post-UV irradiation (40 J/m<sup>2</sup>), the cells were fixed and double-stained with anti-6-4PP and anti-pATM (Ser<sup>1981</sup>) or anti-pChk2 (Thr<sup>68</sup>) antibodies.

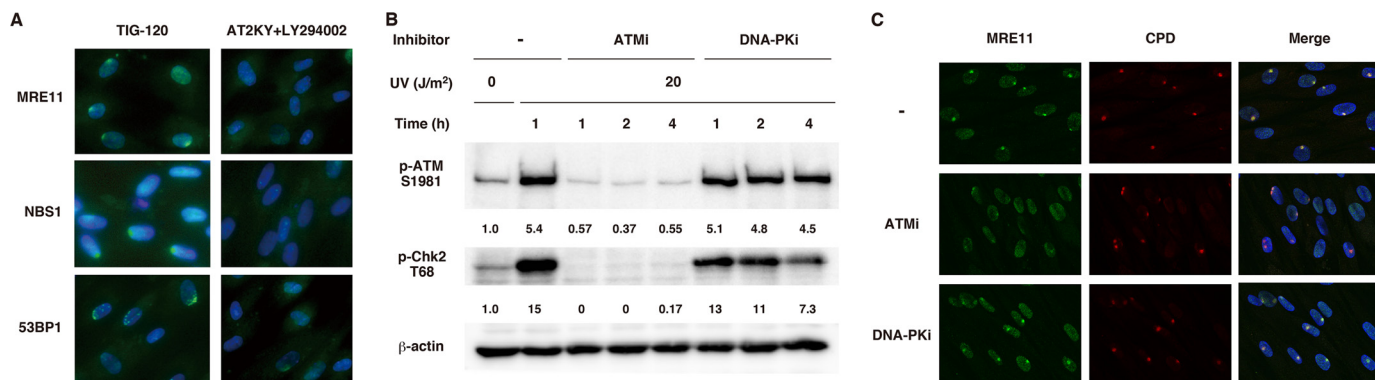


**FIGURE 2. The NER-dependent recruitment of DDR factors mainly depends on ATM activity.** A, TIG-120 or AT2KY cells were arrested in G<sub>0</sub> phase and locally irradiated with 40 J/m<sup>2</sup> of UV through an isopore membrane filter (pore size, 8 μm). After 1-h incubation, the cells were fixed and immunostained with the indicated antibodies. Note that AT2KY cells were treated with 100 μM LY294002 for 30 min before UV irradiation and during post-UV 1-h incubation. B, G<sub>0</sub>-arrested TIG-120 cells were pretreated with or without either 10 μM KU-55933 (ATMi) or 10 μM NU7026 (DNA-PKi) for 30 min. The cells were irradiated with 20 J/m<sup>2</sup> of UV and incubated with or without each inhibitor for 1–4 h before cell lysis. The phosphorylation of ATM and Chk2 was analyzed by Western blotting with phospho-specific antibodies to Ser<sup>1981</sup> and Thr<sup>68</sup>, respectively. C, G<sub>0</sub>-arrested TIG-120 cells were pretreated with ATMi or DNA-PKi as described above and locally irradiated with 40 J/m<sup>2</sup> of UV through an isopore membrane filter (pore size, 5 μm). After 1-h incubation with each inhibitor, the cells were co-immunostained with anti-MRE11 and anti-CPD antibodies.

(A and B), SuSa/T-n cells exhibited elongated comet tails following UV and a dose-dependent increase of tail moment. In clear contrast, NER-deficient XP3OS/T-n (XP-A) cells failed to show the elongation of comet tails (Fig. 3, B and C). These results strongly suggest that DSB is indeed generated in UV-irradiated quiescent cells in an NER-dependent manner.

*ATM Partly Contributes to UV-induced H2AX Phosphorylation as Well as UV Resistance in Quiescent Human Cells*—The findings of NER-dependent DSB formation and ATM activation 1 h post-UV in quiescent cells prompted us to test whether the early fraction of UV-induced H2AX phosphorylation is mediated by ATM. G<sub>0</sub>-arrested TIG-120 cells were pretreated

## NER-dependent DSB Formation and ATM Activation in G<sub>0</sub> Phase

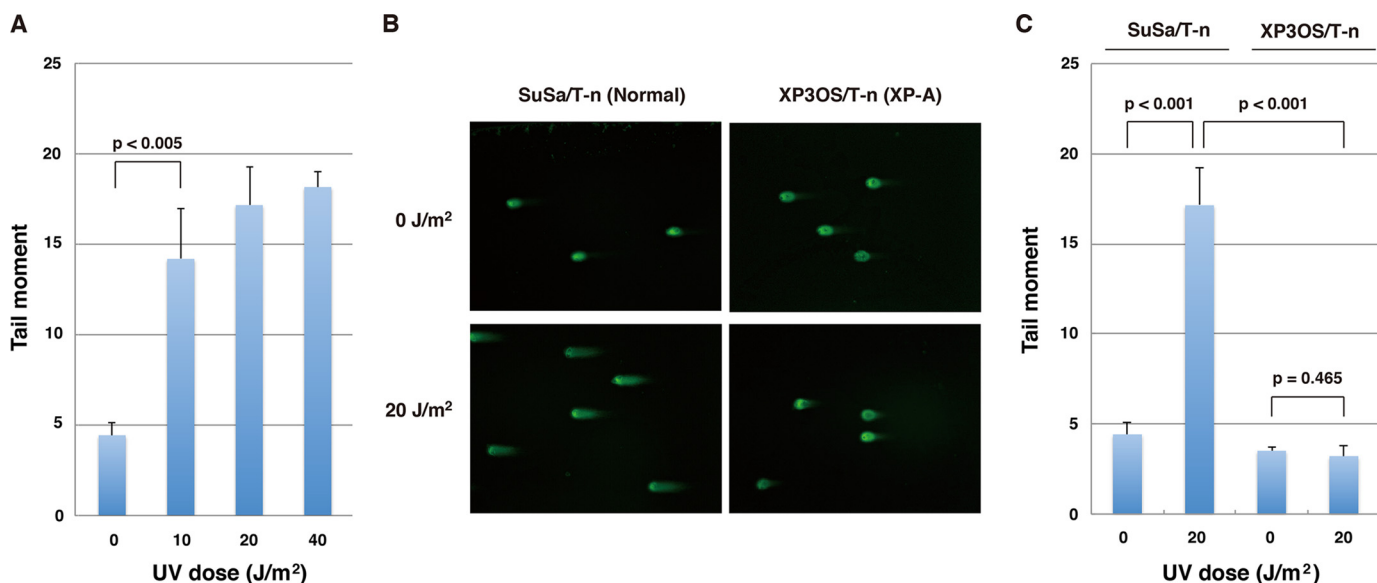


**FIGURE 3. NER-dependent DSB formation in quiescent human cells.** *A*, G<sub>0</sub>-arrested SuSa/T-n cells were irradiated with the indicated doses of UV and incubated for 1 h. The cells were processed according to the manufacturer's instructions for the Comet assay kit (Trevigen), and tail moment was calculated using a CometScore™ program (TriTek Corp.). The mean values of tail moment with standard deviations were plotted as histograms. The statistical differences were determined by Student's *t* test. *B* and *C*, G<sub>0</sub>-arrested SuSa/T-n or XP3OS/T-n cells were irradiated with 20 J/m<sup>2</sup> of UV and incubated for 1 h. DSB formation was analyzed by the neutral comet assay as described above. The representative images and quantitative data from three independent experiments were shown in *B* and *C*, respectively.

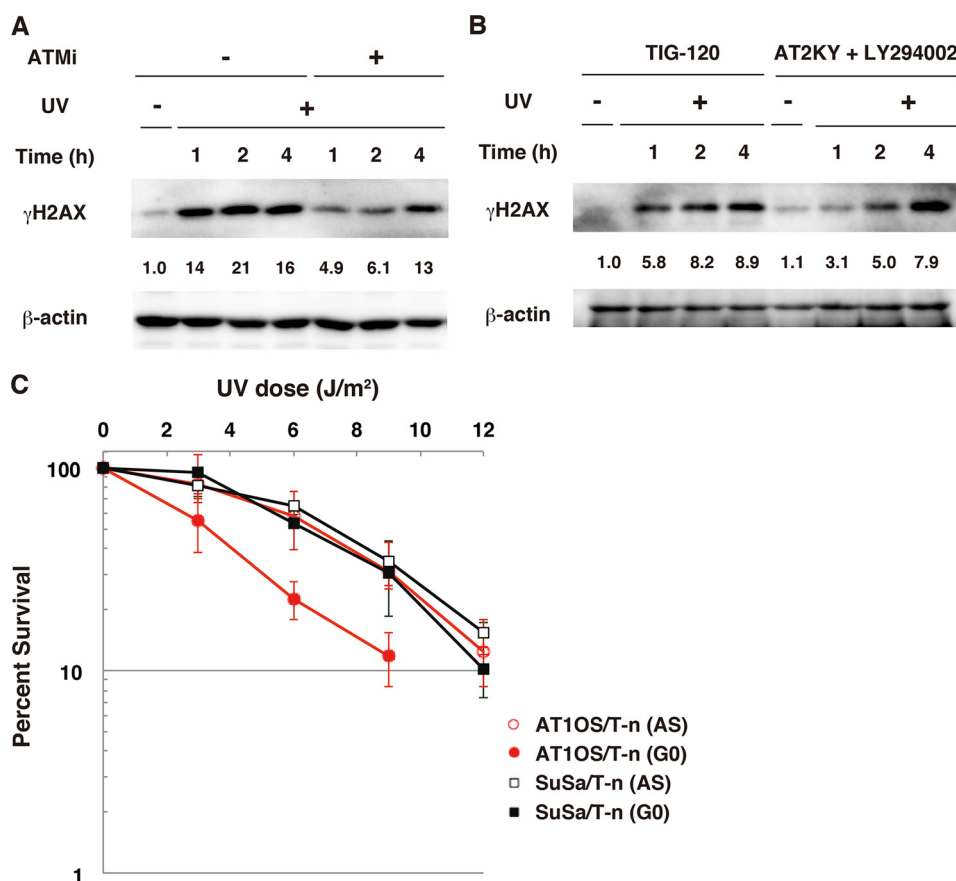


**FIGURE 4. Partial contribution of ATM to UV-induced H2AX phosphorylation and UV resistance in quiescent human cells.** *A*, G<sub>0</sub>-arrested TIG-120 cells were pretreated with ATMi as described in the legend to Fig. 2 and irradiated with 20 J/m<sup>2</sup> of UV. After incubation with ATMi for the indicated periods, cell lysates were prepared and analyzed by Western blotting with anti-γH2AX antibody. *B*, G<sub>0</sub>-arrested AT2KY cells were treated with LY294002 as described in Fig. 2. The cells were irradiated with 20 J/m<sup>2</sup> of UV, and the phosphorylation of H2AX was analyzed by Western blotting. *C*, asynchronously growing (AS) or G<sub>0</sub>-arrested SuSa/T-n or AT1OS/T-n cells were plated into 60-mm dishes and irradiated with the indicated doses of UV after 6-h incubation. The cells were further incubated for 2–3 weeks, and the resultant colonies were counted after ethanol fixation and Giemsa staining.

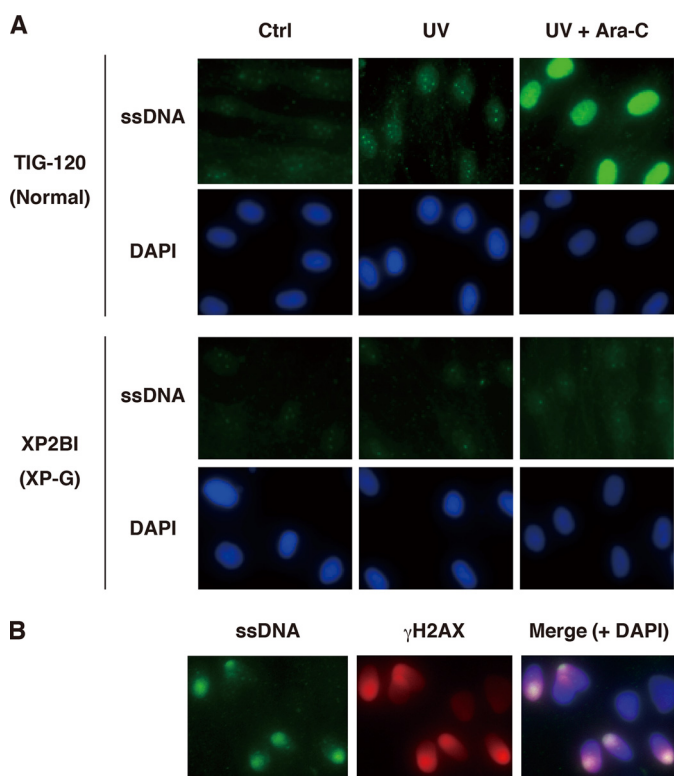


FIGURE 5. **NER-dependent ssDNA formation in quiescent human cells.** *A*, G<sub>0</sub>-arrested TIG-120 or XP2BI cells were irradiated with 40 J/m<sup>2</sup> of UV and incubated for 4 h in the absence or presence of 100 μM Ara-C. After treatment with 0.5% Triton X-100, cells were fixed with methanol/acetone and stained with anti-ssDNA antibody and DAPI. *B*, G<sub>0</sub>-arrested TIG-120 cells were locally irradiated with 40 J/m<sup>2</sup> of UV through an isopore membrane filter (pore size, 8 μm) and incubated for 4 h in the presence of Ara-C. The cells were fixed as described above and co-stained with anti-ssDNA and anti-γH2AX antibodies. *Ctrl*, control.

with KU-55933 and exposed to 20 J/m<sup>2</sup> of UV. Following 1–4 h of incubation, their lysates were prepared and analyzed by Western blotting with anti-γH2AX antibody (Fig. 4A). As expected, the ATM inhibitor markedly attenuated UV-induced H2AX phosphorylation at 1 and 2 h, but not 4 h. We also obtained the similar observation using a pair of TIG-120 cells and LY294002-treated AT2KY cells (Fig. 4B). These results clearly indicate that ATM contributes to the earlier fraction of UV-induced H2AX phosphorylation.

On the other hand, the latter fraction of H2AX phosphorylation (*i.e.* 4 h post-UV) is likely to be mediated by ATR in response to ssDNA (14). We tried to detect ssDNA formation in G<sub>0</sub>-arrested TIG-120 cells exposed to UV by immunostaining with anti-ssDNA antibody. As shown in Fig. 5A, immunofluorescence signals in the nuclei were increased 4 h post-UV and further enhanced by the addition of Ara-C, which blocks a gap-filling step of NER. Importantly, those signals were undetectable in NER-deficient XP2BI (XP-G) cells even in the presence of Ara-C. In addition, locally UV-irradiated TIG-120 cells revealed that ssDNA regions are merged with γH2AX signals (Fig. 5B). Taken together, we conclude that in quiescent cells, NER reaction potentially generates at least two kinds of secondary DNA damage: DSB and ssDNA.

To explore the contribution of ATM signaling to UV resistance in quiescent cells, we employed a clonogenic survival assay. For this assay, hTERT-immortalized cell lines, SuSa/T-n

(normal) and AT1OS/T-n (A-T), were used because of higher colony forming ability than primary fibroblasts. Asynchronously growing or G<sub>0</sub>-arrested cells were plated into dishes and irradiated with various doses of UV before colony formation. Both cell lines showed similar UV sensitivity when exposed under asynchronously growing conditions, consistent with normal NER activity of A-T cells.<sup>5</sup> However, AT1OS/T-n but not SuSa/T-n cells exhibited enhanced UV sensitivity when exposed under quiescent conditions (Fig. 4C). These results strongly suggest that ATM signaling also functions in survival responses of UV-irradiated quiescent cells.

**NER-dependent H2AX Phosphorylation in Quiescent Cell Populations *in Vivo***—Given that NER-dependent secondary DNA lesions (*i.e.* ssDNA and DSB) are generated in cultured quiescent cells, we wished to know whether this is also the case in quiescent cell populations *in vivo*. To test this possibility, T lymphocytes were isolated from lymph nodes or thymus of C57BL/6 mice and exposed to UV. Flow cytometric analyses with anti-γH2AX antibody revealed efficient H2AX phosphorylation in T lymphocytes from lymph nodes but not thymus, whereas etoposide-induced phosphorylation was comparably detected in both T cell populations (Fig. 6A). The inefficient H2AX phosphorylation in thymus-derived T lymphocytes might be explained by higher levels of DNA polymerase δ/ε and PCNA (Fig. 6B). On the other hand, lymph node-derived T lymphocytes isolated from NER-deficient xpa knock-out mice exhibited no UV-induced H2AX phosphorylation by flow cytometric (Fig. 6C) and Western blot (Fig. 6D) analyses, although there was efficient phosphorylation after etoposide treatment. Taken together, these results suggest that NER-dependent secondary DNA damage formation also occurs in quiescent cell populations *in vivo*.

## DISCUSSION

In this study, we have found that DSB is also generated in quiescent cells exposed to UV in an NER-dependent manner (Fig. 3), in addition to ssDNA regions (Fig. 5) (14). The NER-mediated DSB formation is relatively rapid compared with ssDNA formation, leading to the activation of ATM kinase (Fig. 1, B and C) and the recruitment of its downstream factors, NBS1, MRE11, MDC1, and 53BP1 (Figs. 1A and 2A) within 1 h post-UV. Consistently, the earlier fraction of UV-induced H2AX phosphorylation is dependent on ATM activity (Fig. 4A). In the literature, UV-induced activation of ATM and its downstream reactions have been shown by several groups (25–27). In those studies, however, asynchronous cell populations were used, and thus the activation of ATM signaling is likely caused by replication fork stalling and/or DSB formation resulting from replication fork collapse, but not by NER.

Although NBS1, MRE11, MDC1, and 53BP1 are well known DDR factors involved in ATM signaling (2, 5, 21), they are also known to function in ATR signaling. The MRE11-RAD50-NBS1 complex acts both upstream and downstream of ATR to regulate the S phase checkpoint following UV (28). Moreover, Jeggo and co-workers (29) reported that replication-independent ATR signaling requires NBS1, 53BP1, and MDC1, but not H2AX, to induce G<sub>2</sub>/M arrest. Recently, MDC1 was reported to accumulate at locally UV-damaged subnuclear regions in an

## NER-dependent DSB Formation and ATM Activation in G<sub>0</sub> Phase

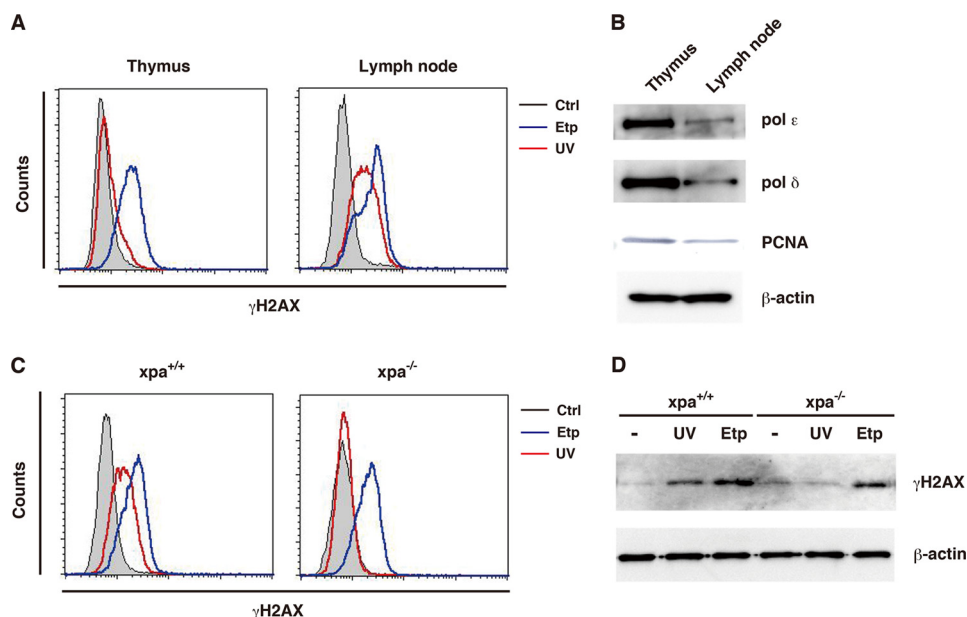


**FIGURE 6. UV-induced H2AX phosphorylation in peripheral T lymphocytes in an NER-dependent manner.** *A*, T lymphocytes isolated from thymus or lymph nodes of C57BL/6 mice were exposed to 20 J/m<sup>2</sup> of UV and incubated for 1 h or treated with 40 μg/ml of etoposide for 1 h. The cells were stained with anti-γH2AX antibody and propidium iodide and analyzed by flow cytometry. *B*, cell lysates were prepared from the isolated T lymphocytes and analyzed by Western blotting with the indicated antibodies. *C* and *D*, peripheral T lymphocytes from lymph nodes of wild-type or *xpa* knock-out mice were treated with UV or etoposide and analyzed for H2AX phosphorylation by flow cytometry (*C*) or Western blotting (*D*) with anti-γH2AX antibody. *Ctrl*, control; *Etp*, etoposide; *pol*, polymerase.

NER- and ATR-dependent manner, which recruits RNF8 ubiquitinating histone H2A and hereby 53BP1 and BRCA1 (30). In our experiments, however, local accumulation of MRE11 after micropore UV irradiation was markedly diminished by KU-55933 (Fig. 2C), suggesting downstream reactions of ATM signaling rather than ATR signaling.

The NER reaction generates ~30-nucleotide ssDNA gap intermediates by making dual incisions by XPF-ERCC1 (5') and XPG (3') endonucleases (17, 31–35). It might be possible that two events of dual incisions in close proximity on different DNA strands generates DSB, but this would be unlikely at UV doses used in this study, as discussed by others in detail (12). Another possibility is that some endonuclease(s) might be involved in the NER-dependent DSB formation. Similarly, it is plausible that NER-mediated ssDNA gaps in quiescent cells may need additional enzymatic processing to activate ATR for H2AX phosphorylation. In fact, ATR-mediated checkpoint activation has been shown to require the gap enlargement of NER intermediates by Exo1, using yeast Exo1 mutant (36), Exo1-down-regulated human cell lines (37), or more clearly a defined *in vitro* system (38). The mechanism underlying the NER-dependent DSB formation is currently unknown and awaits further study.

Cleaver and co-workers have reported that H2AX phosphorylation in cycling G<sub>1</sub> phase cells exposed to UV depends on NER but not DSB (12), although a minority of UV-induced γH2AX signal in S phase contains DSB (39). The NER-mediated DSB formation might be a specific or more frequent event in G<sub>0</sub> phase cells compared with cycling G<sub>1</sub> phase cells. In other words, quiescent cells need to activate not only NER but also other DDR pathways including ATR/ATM signaling and other DNA repair systems. Consistently, we found that functional

ATM positively contributes to survival responses in quiescent cells exposed to UV (Fig. 4C).

The majority of *in vivo* cells are known to be nonproliferating or extremely slow to divide (*e.g.* terminally differentiated cells, tissue stem cells, and so on) (40). The NER-dependent H2AX phosphorylation can be observed after not only UV irradiation but also the treatment with *N*-acetoxy-2-acetylaminofluorene (14) or cisplatin<sup>5</sup> that produces bulky base adducts or intrastand cross-links repairable by NER. The *in vivo* quiescent cells possibly suffer from the NER-mediated secondary DNA damage, in addition to initial base damage generated by UV or chemicals, and need to activate the multiple DDR mechanisms to prevent cell death or carcinogenic mutation.

*Acknowledgments*—We thank Dr. Kanji Ishizaki (Aichi Cancer Center Research Institute) for the hTERT-transformed cell lines and Dr. Toshio Mori (Nara Medical University) for XP2BI cells. We also thank Dr. Kuniyoshi Iwabuchi (Kanazawa Medical University) for anti-53BP1 antibody and Ai Igarashi for technical assistance.

## REFERENCES

1. Sancar, A., Lindsey-Boltz, L. A., Unsal-Kaçmaz, K., and Linn, S. (2004) Molecular mechanisms of mammalian DNA repair and the DNA damage checkpoints. *Annu. Rev. Biochem.* **73**, 39–85
2. Ciccia, A., and Elledge, S. J. (2010) The DNA damage response: Making it safe to play with knives. *Mol. Cell* **40**, 179–204
3. Jackson, S. P., and Bartek, J. (2009) The DNA-damage response in human biology and disease. *Nature* **461**, 1071–1078
4. Downs, J. A., Nussenzweig, M. C., and Nussenzweig, A. (2007) Chromatin dynamics and the preservation of genetic information. *Nature* **447**, 951–958
5. van Attikum, H., and Gasser, S. (2009) Crosstalk between histone modifications during the DNA damage response. *Trends Cell Biol.* **19**, 207–217

6. Bonner, W. M., Redon, C. E., Dickey, J. S., Nakamura, A. J., Sedelnikova, O. A., Solier, S., and Pommier, Y. (2008)  $\gamma$ H2AX and cancer. *Nat. Rev. Cancer* **8**, 957–967
7. Friedberg E. C., Walker G. C., Siede W., Wood R. D., Schultz R. A., and Ellenberger T. (2006) *DNA Repair and Mutagenesis*, ASM Press, Washington, D.C.
8. Ward, I. M., and Chen, J. (2001) Histone H2AX is phosphorylated in an ATR-dependent manner in response to replicational stress. *J. Biol. Chem.* **276**, 47759–47762
9. Cimprich, K. A., and Cortez, D. (2008) ATR: an essential regulator of genome integrity. *Nat. Rev. Mol. Cell Biol.* **9**, 616–627
10. Flynn, R. L., and Zou, L. (2011) ATR: a master conductor of cellular responses to DNA replication stress. *Trends Biochem. Sci.* **36**, 133–140
11. O'Driscoll, M., Ruiz-Perez, V. L., Woods, C. G., Jeggo, P. A., and Goodship, J. A. (2003) A splicing mutation affecting expression of ataxia-telangiectasia and Rad3-related protein (ATR) results in Seckel syndrome. *Nat. Genet.* **33**, 497–501
12. Marti, T. M., Hefner, E., Feeney, L., Natale, V., and Cleaver, J. E. (2006) H2AX phosphorylation within the G1 phase after UV irradiation depends on nucleotide excision repair and not DNA double-strand breaks. *Proc. Natl. Acad. Sci. U.S.A.* **103**, 9891–9896
13. Hanasoge, S., and Ljungman, M. (2007) H2AX phosphorylation after UV irradiation is triggered by DNA repair intermediates and is mediated by the ATR kinase. *Carcinogenesis* **28**, 2298–2304
14. Matsumoto, M., Yaginuma, K., Igarashi, A., Imura, M., Hasegawa, M., Iwabuchi, K., Date, T., Mori, T., Ishizaki, K., Yamashita, K., Inobe, M., and Matsunaga, T. (2007) Perturbed gap-filling synthesis in nucleotide excision repair causes histone H2AX phosphorylation in human quiescent cells. *J. Cell Sci.* **120**, 1104–1112
15. Vrouwe, M. G., Pines, A., Overmeer, R. M., Hanada, K., and Mullenders, L. H. (2011) UV-induced photolesions elicit ATR-kinase-dependent signaling in non-cycling cells through nucleotide excision repair-dependent and -independent pathways. *J. Cell Sci.* **124**, 435–446
16. Sancar, A. (1996) DNA excision repair. *Annu. Rev. Biochem.* **65**, 43–81
17. Huang, J.-C., Svoboda, D. L., Reardon, J. T., and Sancar, A. (1992) Human nucleotide excision nuclease removes thymine dimers from DNA by incising the 22nd phosphodiester bond 5' and the 6th phosphodiester bond 3' to the photodimer. *Proc. Natl. Acad. Sci. U.S.A.* **89**, 3664–3668
18. Wood, R. D. (1996) DNA repair in eukaryotes. *Annu. Rev. Biochem.* **65**, 135–167
19. Bootsma, D., Kraemer, K. H., Cleaver, J. E., and Hoeijmakers, J. H. J. (1998) Nucleotide excision repair syndromes: xeroderma pigmentosum, Cockayne syndrome and trichothiodystrophy. In *The Genetic Basis of Human Cancer* (Vogelstein, B., and Kinzler, K. W., eds) pp. 245–274, McGraw-Hill Inc., New York
20. Mori, T., Nakane, M., Hattori, T., Matsunaga, T., Ihara, M., and Nikaido, O. (1991) Simultaneous establishment of monoclonal antibodies specific for either cyclobutane pyrimidine dimer or (6-4)photoproduct from the same mouse immunized with ultraviolet-irradiated DNA. *Photochem. Photobiol.* **54**, 225–232
21. Bekker-Jensen, S., and Mailand, N. (2010) Assembly and function of DNA double-strand break repair foci in mammalian cells. *DNA Repair* **9**, 1219–1228
22. Nakamura, H., Fukami, H., Hayashi, Y., Kiyono, T., Nakatsugawa, S., Hamaguchi, M., and Ishizaki, K. (2002) Establishment of immortal normal and ataxia telangiectasia fibroblast cell lines by introduction of the hTERT gene. *J. Radiat. Res.* **43**, 167–174
23. Stiff, T., O'Driscoll, M., Rief, N., Iwabuchi, K., Löbrich, M., and Jeggo, P. A. (2004) ATM and DNA-PK function redundantly to phosphorylate H2AX after exposure to ionizing radiation. *Cancer Res.* **64**, 2390–2396
24. Suzuki, K., Kodama, S., and Watanabe, M. (1999) Recruitment of ATM protein to double strand DNA irradiated with ionizing radiation. *J. Biol. Chem.* **274**, 25571–25575
25. Stiff, T., Walker, S. A., Cersaletti, K., Goodarzi, A. A., Petermann, E., Concannon, P., O'Driscoll, M., and Jeggo, P. A. (2006) ATR-dependent phosphorylation and activation of ATM in response to UV treatment or replication fork stalling. *EMBO J.* **25**, 5775–5782
26. Yajima, H., Lee, K. J., Zhang, S., Kobayashi, J., and Chen, B. (2009) DNA double-strand break formation upon UV-induced replication stress activates ATM and DNA-PKcs kinases. *J. Mol. Biol.* **385**, 800–810
27. Oh, K.-S., Bustin, M., Mazur, S. J., Appella, E., and Kraemer, K. H. (2011) UV-induced histone H2AX phosphorylation and DNA damage related proteins accumulate and persist in nucleotide excision repair-deficient XP-B cells. *DNA Repair* **10**, 5–15
28. Olson, E., Nievera, C. J., Lee, A. Y., Chen, L., and Wu, X. (2007) The Mre11-Rad50-Nbs1 complex acts both upstream and downstream of ataxia telangiectasia mutated and Rad3-related protein (ATR) to regulate the S-phase checkpoint following UV treatment. *J. Biol. Chem.* **282**, 22939–22952
29. Stiff, T., Cersaletti, K., Concannon, P., O'Driscoll, M., and Jeggo, P. A. (2008) Replication independent ATR signaling leads to G2/M arrest requiring Nbs1, 53BP1 and MDC1. *Hum. Mol. Genet.* **17**, 3247–3253
30. Martejijn, J. A., Bekker-Jensen, S., Mailand, N., Lans, H., Schwertman, P., Gourdin, A. M., Dantuma, N. P., Lukas, J., and Vermeulen, W. (2009) Nucleotide excision repair-induced H2A ubiquitination is dependent on MDC1 and RNF8 and reveals a universal DNA damage response. *J. Cell Biol.* **186**, 835–847
31. O'Donovan, A., Davies, A. A., Moggs, J. G., West, S. C., and Wood, R. D. (1994) XPG endonuclease makes the 3' incision in human DNA nucleotide excision repair. *Nature* **371**, 432–435
32. Matsunaga, T., Mu, D., Park, C.-H., Reardon, J. T., and Sancar, A. (1995) Human DNA repair excision nuclease analysis of the roles of the subunits involved in dual incisions by using anti-XPG and anti-ERCC1 antibodies. *J. Biol. Chem.* **270**, 20862–20869
33. Mu, D., Hsu, D. S., and Sancar, A. (1996) Reaction mechanism of human DNA repair excision nuclease. *J. Biol. Chem.* **271**, 8285–8294
34. Sijbers, A. M., de Laat, W. L., Ariza, R. R., Biggerstaff, M., Wei, Y. F., Moggs, J. G., Carter, K. C., Shell, B. K., Evans, E., de Jong, M. C., Rademakers, S., de Rooij, J., Jaspers, N. G., Hoeijmakers, J. H., and Wood, R. D. (1996) Xeroderma pigmentosum group F caused by a defect in a structure-specific DNA repair endonuclease. *Cell* **86**, 811–822
35. Reardon, J. T., Thompson, L. H., and Sancar, A. (1997) Rodent UV-sensitive mutant cell lines in complementation groups 6–10 have normal general excision repair activity. *Nucleic Acids Res.* **25**, 1015–1021
36. Giannattasio, M., Follonier, C., Tourrière, H., Puddu, F., Lazzaro, F., Passero, P., Lopes, M., Plevani, P., and Muzi-Falconi, M. (2010) Exo1 competes with repair synthesis, converts NER intermediates to long ssDNA gaps, and promotes checkpoint activation. *Mol. Cell* **40**, 50–62
37. Sertic, S., Pizzi, S., Cloney, R., Lehmann, A. R., Marini, F., Plevani, P., and Muzi-Falconi, M. (2011) Human exonuclease 1 connects nucleotide excision repair (NER) processing with checkpoint activation in response to UV irradiation. *Proc. Natl. Acad. Sci. U.S.A.* **108**, 13647–13652
38. Lindsey-Boltz, L. A., Kemp, M. G., Reardon, J. T., DeRocco, V., Iyer, R. R., Modrich, P., and Sancar, A. (2014) Coupling of human DNA excision repair and the DNA damage checkpoint in a defined in vitro system. *J. Biol. Chem.* **289**, 5074–5082
39. de Feraudy, S., Revet, I., Bezroukove, V., Feeney, L., and Cleaver, J. (2010) A minority of foci or pan-nuclear apoptotic staining of  $\gamma$ H2AX in the S phase after UV damage contain DNA double-strand breaks. *Proc. Natl. Acad. Sci. U.S.A.* **107**, 6870–6875
40. Pietras, E. M., Warr, M. R., and Passegué, E. (2011) Cell cycle regulation in hematopoietic stem cells. *J. Cell Biol.* **195**, 709–720